

# Application of Data Compression Methods to the Redshift-space distortions of the PSCz galaxy catalogue

A.N. Taylor<sup>\*</sup>, W.E. Ballinger<sup>†</sup>, A.F. Heavens<sup>\*</sup>, H. Tadros<sup>†</sup>

<sup>\*</sup>*Institute for Astronomy, University of Edinburgh, Royal Observatory, Blackford Hill, Edinburgh, U.K.*

<sup>†</sup>*Astrophysics, University of Oxford, Keble Road, Oxford OX1 3RH*

*ant@roe.ac.uk, ballinger@astro.ox.ac.uk, afh@roe.ac.uk, h.tadros1@physics.oxford.ac.uk*

30 October 2018

## ABSTRACT

We apply a spherical harmonic analysis to the Point Source Redshift Survey (PSCz), to compute the real-space galaxy power spectrum and the degree of redshift distortion caused by peculiar velocities. We employ new parameter eigenvector and hierarchical data compression techniques, allowing a much larger number of harmonic modes to be included, and correspondingly smaller error bars. Using 4644 harmonic modes, compressed to 2278, we find that the IRAS redshift-space distortion parameter is  $\beta = 0.39 \pm 0.12$  and the amplitude of galaxy clustering on a scale of  $k = 0.1 \text{ hMpc}^{-1}$  is  $\Delta_{\text{gal}}(0.1) = 0.42 \pm 0.02$ . Combining these we find the amplitude of mass perturbations is  $\Delta_m(0.1) = (0.16 \pm 0.04)\Omega_m^{-0.6}$ . A preliminary model fitting analysis combining the PSCz amplitudes with the CMB and abundance of clusters yields the cosmological matter density parameter  $\Omega_m = 0.16 \pm 0.03$ , the amplitude of primordial perturbations  $Q = (8.4 \pm 3.8) \times 10^{-5}$ , and the IRAS bias parameter  $b = 0.84 \pm 0.28$ .

**Key words:** large-scale structure of the Universe

## 1 INTRODUCTION

The extraction of cosmological parameters from surveys has entered a new phase, with the advent of very large data sets. But the prospect of accurately determining a wide range of parameters is offset by the difficult task of manipulating these large data sets without losing important parameter information. In the case of analysing near-all sky redshift surveys we have developed a method based on the harmonic decomposition of the survey into spherical harmonics and radial spherical Bessel functions (Heavens & Taylor 1995, Ballinger, Heavens & Taylor 1995, Tadros et al 1999; hereafter HT, BHT and T99, respectively). The use of a spherical harmonic decomposition allows the accurate analysis of the radial redshift-space distortion effect, without using the small-angle or distant observer approximations, and the natural inclusion of angular and radial window functions. The parameters of interest are the degree of redshift-space distortion, parameterised by<sup>\*</sup>

$$\beta \equiv \frac{f(\Omega_m)}{b} \quad (1)$$

<sup>\*</sup> Since differently selected galaxies cluster differently, each selection may have its own bias parameter and  $\beta$ . In this paper we shall use  $\beta$  and  $b$  to refer exclusively to IRAS selected galaxies.

where  $f(\Omega_m) = d \ln \delta / d \ln a \approx \Omega_m^{0.6}$  (Peebles 1980) is the growth rate of perturbations and  $b$  is the linear bias parameter defined by

$$P_{\text{gal}}(k) = b^2 P_m(k), \quad (2)$$

and an estimate of the undistorted galaxy power spectrum,  $P_{\text{gal}}(k)$ . This approach combines the spherical harmonic decomposition with a mode-by-mode maximum likelihood analysis, and has been applied to the 1.2Jy survey, a 1:6 subsample of the IRAS galaxy survey (HT, BHT) and the full 1:1 sample, the PSCz (T99). T99 used the most sophisticated analysis to date, and found a distortion parameter of  $\beta = 0.58 \pm 0.26$  (marginal error) and an amplitude for the real space galaxy power spectrum at  $k = 0.1 \text{ hMpc}^{-1}$  of  $\Delta_{0.1} = 0.42 \pm 0.03$ , where  $\Delta^2(k) = k^3 P(k) / 2\pi^2$ . In this paper we employ new data compression methods to improve on this analysis and obtain more accurate parameter determinations. We describe the methods more fully in Ballinger et al (2000).

The limiting factors in our previous analyses were CPU time and stability. To complete the likelihood analysis the data covariance matrix of the full data set must be inverted at each point in parameter space. Small numerical errors can make this procedure unstable; data compression (Section 2) is a great help here, as the high signal-to-noise modes are well-behaved. The CPU factor can also be an issue when one wishes to investigate systematic effects in data sets. This

is as much an issue in analysis of the Cosmic Microwave Background (CMB) as it is in galaxy redshift surveys, such as the PSCz, the 2-degree Field (2dF) or the Sloan Digital Sky Survey (SDSS).

The problem of analysing large data sets was addressed by Tegmark, Taylor & Heavens (1997; TTH) who considered the question of what was the optimal transformation of the data for estimating a given parameter, where the model data covariance matrix could be an arbitrary, nonlinear function of the desired parameter. The optimal transformation should have the properties of maximising the information content about the parameter in the minimum number of eigenmodes. By ordering modes the ones with the most information could be selected and the rest discarded. That the data can be ordered this way can be understood if one considers that the data may contain noisy or strongly correlated modes that add little information about the parameter of interest. Choosing the transformed data to have diagonal covariance also decreases the computation time. While the data covariance is only diagonal at one point in parameter space, the removal of correlated and noisy data by trimming produces a numerically stable inversion of the covariance matrix.

This procedure sounds similar to Principle Component Analysis (PCA) or signal-to-noise eigenvalue analysis (SNA; Bond 1995, Vogeley & Szalay 1995), but has important differences. We have previously referred to the procedure as Karhunen-Loève methods, but it is in fact more general, so we shall refer to our method henceforth as Optimal-Mode Analysis (OMA). In this paper, we introduce two new methods for accurate parameter estimation, and refer to the whole method as *Generalised Optimal Mode Analysis*, or GOMA.

The additional features of GOMA can be split into two parts, dealing with multiparameter estimation and the stable handling of data compression. In multiparameter estimation it is useful to note that for highly-correlated multiparameter estimates (highly-elongated likelihood surfaces, not aligned with parameter axes), the marginal error in the parameters is determined by the length of the longest likelihood principal axis. We therefore want to optimise to keep this length as short as possible. This process is called *parameter eigenmode analysis*, and was introduced in Ballinger (1997), with some results being presented in Taylor et al. (1997). The second, optional part of GOMA is to split the original data into subsets, optimising each subset, and then combining the best modes together. This procedure can be used hierarchically, to reduce a very large number of modes to a manageable size. This process we refer to as *hierarchical data compression*. These methods will be detailed in a companion paper (Ballinger et al. 2000).

In this paper we combine our spherical harmonic decomposition, parameter eigenmode analysis and hierarchical data compression methods to analyse the PSCz. We study both nonlinear multiparameter estimation, the redshift-space distortion parameter and the amplitude of power, using hierarchical data compression, from the harmonic modes of the PSCz survey. The increase in analysing power using these methods allows us to increase the number of modes available for study, and hence a corresponding increase in accuracy of our results.

Padmanabhan, Tegmark and Hamilton (1999) have also used the spherical harmonic decomposition to analyse the

CFA/SSRS UZC galaxy redshift survey, while Hamilton, Tegmark & Padmanabhan (2000) have applied the analysis to the PSCz redshift survey. In both cases they employ Karhunen-Loève methods to estimate the quadratic band-power in these surveys. In the former survey the band-power was measured in redshift-space, while in the latter analysis of the PSCz they measured the real-space galaxy-galaxy, galaxy-velocity and velocity-velocity power spectra, and estimated  $\beta$  from a least squares fit to the ratios of the galaxy-velocity to galaxy-galaxy and velocity-velocity to galaxy-galaxy power spectra.

The paper can be summarised as follows. In Section 2 we briefly review the spherical harmonic decomposition, OMA, parameter eigenmodes and hierarchical data compression methods. In Section 3 we perform a maximum likelihood analysis of the PSCz, for the redshift-space distortion parameter and real-space clustering amplitude of galaxies. Our results are presented in Section 4, and conclusions are made in Section 5. We begin by a brief review of our data analysis methods.

## 2 DATA ANALYSIS

### 2.1 Spherical Harmonic decomposition

Following HT, BHT, and T99 we can decompose the density field of galaxies in a redshift survey into harmonic modes

$$\rho_{\ell mn} = c_{\ell n} \int d^3s \rho(\mathbf{s}) w(s) j_\ell(ks) Y_{\ell m}^*(\Omega), \quad (3)$$

where  $Y_{\ell m}$ , are spherical harmonics,  $j_\ell$  are a discrete set of spherical Bessel functions,  $w(s)$  is an adjustable weighting function and  $\mathbf{s}$  is the redshift-space position variable. The  $c_{\ell n}$  are normalization constants and  $k = k_{\ell n}$  are discrete wavenumbers. Each mode was weighted with a Feldmann-Kaiser-Peacock (1994) weight,  $w(k, s) = [1 + \phi(s)P(k)]^{-1}$ , where  $\phi(s)$  is the (redshift-dependent) average number density of galaxies in the survey.

The observed coefficients,  $D_{\ell mn}$ , can be related to the underlying linear density modes,  $\delta_{\ell mn}$ , by (HT, BHT, T99)

$$\mathbf{D} \equiv \rho - \rho_0 = \mathbf{S}\mathbf{W}(\mathbf{\Phi} + \beta\mathbf{V})\boldsymbol{\delta}. \quad (4)$$

The transition matrices  $\mathbf{S}$ ,  $\mathbf{W}$ ,  $\mathbf{\Phi}$  and  $\mathbf{V}$  correspond to the effects of small-scale random radial velocity distortions, the angular window function, the radial galaxy selection function and linear redshift space distortions, respectively. The mean field,  $\rho_0$ , is nonzero due to the radial selection function and angular window function. Note that there is no matrix multiplication implied between the angular matrix,  $\mathbf{W}$ , and the radial matrix,  $\mathbf{\Phi} + \beta\mathbf{V}$ , since these are orthogonal.

The small-scale radial velocities can be accurately modelled by multiplying the galaxy power spectrum by a Lorentzian function. This implies that each mode is multiplied by the square-root of a Lorentzian. Inverse Fourier transforming we find that the density field should be convolved with the function

$$S(x) = \frac{2\sqrt{2}}{\sigma_v} K_0 \left( \frac{\sqrt{2}}{\sigma_v} x \right), \quad (5)$$

where  $K_n$  is an  $n^{\text{th}}$ -order modified Bessel function and  $\sigma_v$  is the 1-d velocity dispersion. (Note that in the analysis of T99,

the 3-d velocity dispersion was used incorrectly. Changing to the correct value had little effect. However, as we are pushing our model to higher wavenumbers here, it is more important to have the correct value of the velocity dispersion.) The transition matrix,  $\mathbf{S}$ , is found by a spherical harmonic transformation of  $S(x - y)$ .

Two immediate advantages of this treatment are accounting for the effects of the monopole and dipole modes. The monopole mode contains information about the mean density of the survey. In previous methods this can bias down the estimated power as the mean is estimated from the survey itself and may not be the true mean (Tadros & Efstathiou 1996). In our treatment the monopole mode can be removed, effectively removing this bias (T99). As the PSCz is not all sky, some aliasing takes place at the few percent level, and we include the effects of this leakage, through  $\mathbf{W}$ . The dipole includes contributions from our own motion in the redshift space distortion. Again we can mostly remove this by ignoring the dipole mode, and accounting for aliasing from the angular mask (T99).

The distribution of linear harmonic modes can be described by a multivariate likelihood,

$$-2 \ln \mathcal{L}[\mathbf{D}|\beta, P(k)] = \mathbf{D}^t \mathbf{C}^{-1} \mathbf{D} + \ln \det \mathbf{C}, \quad (6)$$

where  $\mathbf{C} = \langle \mathbf{D}\mathbf{D}^t \rangle$  is the data covariance matrix. Details for dealing with non-axisymmetric angular window functions in the covariance matrix, as well as further details of the likelihood analysis, are given in T99.

## 2.2 Generalised Optimal Mode Analysis (GOMA)

The technical advance which allows us to reduce the error bars in the determination of  $\beta$  and the power spectrum is a new optimised form of data compression, which we call generalised optimal mode analysis. Details of the method will appear elsewhere (Ballinger et al. 2000), but we sketch the main ingredients here.

The need for data compression is twofold: first, the speed of analysis generally scales as  $N^3$ , where  $N$  is the number of modes considered. These modes might be, for example, spherical transform coefficients. Secondly, since the covariance matrix is computed numerically, small numerical errors can lead to a non-positive definite matrix, which makes no physical sense; even a single negative eigenvalue out of several thousand is fatal. Instead of working with the full set of spherical transform coefficients up to some maximum wavenumber, we form orthogonal linear combinations, and use these as the data. GOMA consists of two parts; one is *parameter eigenmode analysis*, where instead of choosing  $\beta$  and  $\Delta_{0.1}$  as the two parameters to be determined, we introduce a new parameter, which runs along the longest likelihood ridge of Figure 1, and use the data compression methods of TTH to make the likelihood as narrow as possible in this direction. Since the length of this controls the marginal errors in *both*  $\beta$  and  $\Delta_{0.1}$ , the method is very effective. It is worth noting that only OMA will determine the best set of eigenmodes following this procedure, since we now have a linear combinations of parameters which are nonlinear in the covariance matrix.

The second (optional) ingredient is *hierarchical data compression*. We cannot find the optimal linear combinations of the entire mode set, because of the numerical prob-

lems identified above. Instead, we form optimal orthogonal linear combinations of subsets of the modes (in discrete wavenumber ranges), and then combine the best modes to form a new set. This process can be repeated hierarchically to produce a near-optimal set of modes. Note that when mode sets are combined they are not orthogonal and we use the correct correlation properties.

## 3 APPLICATION TO THE PSCZ

We have applied our methods to the new IRAS PSCz redshift survey (Saunders et al 1999), with a flux cut of 0.75Jy, and the ultra-conservative mask created by T99, corresponding to optical extinctions of  $A_B = 0.75\text{mag}$  and excluding 35% of the sky. Our flux cut is above the formal limit of 0.6Jy for the catalogue, but motivated by a systematic effect we found linked to flux in T99. This appeared as a flux-dependency on the amplitude of real space perturbations, where the low-flux galaxies had roughly a factor of two higher clustering amplitude, the cause of which we were unable to identify. However by cutting the catalogue at 0.75Jy the effect could be removed. This cut in flux, along with the more conservative mask left us with around 7000 galaxies.

The survey was put in a sphere of radius  $r_{\text{max}} = 200 h^{-1}\text{Mpc}$  and transformed into spherical harmonic modes. We analysed all the modes down to  $k = 0.2h\text{Mpc}^{-1}$ , with  $n = 1 - 14$  and  $\ell = 2 - 36$  yielding a total of 4644 harmonic modes. Modes in the range  $n = 0 - 20$  and  $\ell = 0 - 50$  were used for the convolution matrices. Since we use a higher cut in wavenumber,  $k$ , than in the analysis of T99 we must be cautious about introducing nonlinear modes which go beyond our analysis. The main concern is the effect of “fingers-of-god” contaminating our analysis. The effect of these would be to lower the measured value of  $\beta$ , since its effect is to elongate structure along the line of sight, and lower the clustering amplitude. We have tested our methods using CDM simulations under similar conditions, and find that our correction for radial small-scale velocities, equation (5), is accurate (Ballinger et al 2000).

The 4664 modes were compressed down to 2278, using the hierarchical compression method once, and a new likelihood analysis applied. In T99 around 1300 modes were analysed. In this analysis we have partly made use of the increase in computing power in the time between the two analyses. However the real limiting feature of our previous analysis was numerical instability problems in the covariance matrix. Small errors can produce a covariance matrix which is not positive-definite, which makes no physical sense (a probability distribution in data space which grows exponentially along one principal direction). A great advantage of the compression mechanism is that this numerical problem is completely solved: the best modes for parameter estimation are well-behaved, and the covariance matrix inversion proceeds smoothly. Hence the overall time for computing our results (around 1 weeks CPU time) remained constant.

## 4 RESULTS

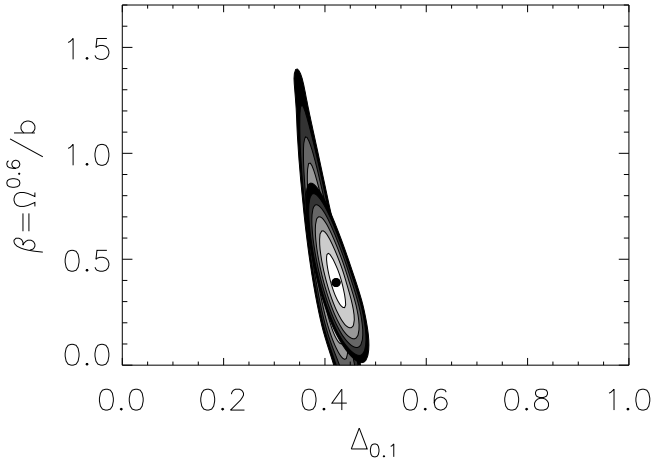


**Figure 1.** Likelihood contours for the parameter space of redshift distortions,  $\beta$ , and real-space galaxy power,  $\Delta_{0.1}$ , measured at  $k = 0.1 h\text{Mpc}^{-1}$  for the PSCz survey cut at a flux limit of  $0.75\text{Jy}$ . The larger set of contours is the results of the Tadros et al (1999) analysis using 1300 modes and  $k_{\text{max}} = 0.13 h\text{Mpc}^{-1}$ . The smaller set of contours is the present analysis using 4644 modes compressed into 2278 modes and  $k_{\text{max}} = 0.20 h\text{Mpc}^{-1}$ . In both analyses a conservative mask was used leaving a total sample of 7042 galaxies. The contours are spaced by  $\Delta \ln \mathcal{L} = -0.5$ .

#### 4.1 Likelihood Analysis

Figure 1 shows the results of our likelihood analysis for the  $\beta - \Delta_{0.1}$  plane. The larger contours are the results of T99 for 1300 modes. Contours are plotted at intervals of  $-0.5$  in  $\ln \mathcal{L}$  from the maximum. The smaller set of contours are for our new analysis for 4644 harmonic modes compressed to 2278. We have used a CDM-type power spectrum with shape parameter  $\Gamma = 0.2$  to calculate the covariance matrices, leaving the amplitude a free parameter, and in the wavenumber-dependent mode weighting function. We used a value of  $\sigma_v = 224 \text{km s}^{-1}$  for the 1-dimensional velocity dispersion of galaxies in the scattering matrices, but have also experimented with  $112 \text{km s}^{-1}$  and  $336 \text{km s}^{-1}$ .

The increase in parameter information yields a new, lower value of

$$\beta = 0.39 \pm 0.12, \quad (7)$$

where we quote the marginalized errors. This is consistent with our previous result, but with a much smaller error ellipse, around a factor of 3 improvement, which significantly rules out both  $\beta = 1$  and  $\beta = 0$ . The amplitude of the real space galaxy power spectrum is

$$\Delta_{0.1} = 0.42 \pm 0.02 \quad (8)$$

which is again consistent with the results of T99 with a slightly smaller error. The covariance parameter of  $\beta$  and  $\Delta_{0.1}$  is  $r = 0.82$ , estimated from the ellipticity of the error ellipse. We find no evidence that our analysis is being biased by nonlinear effects, since then we would expect a sudden change in both the value of  $\beta$  and a drop in the amplitude of real-space perturbations, neither of which is seen. We also find that the maximum likelihood values are almost unchanged, moving by less than  $\Delta\beta \approx 0.1$ , if we change

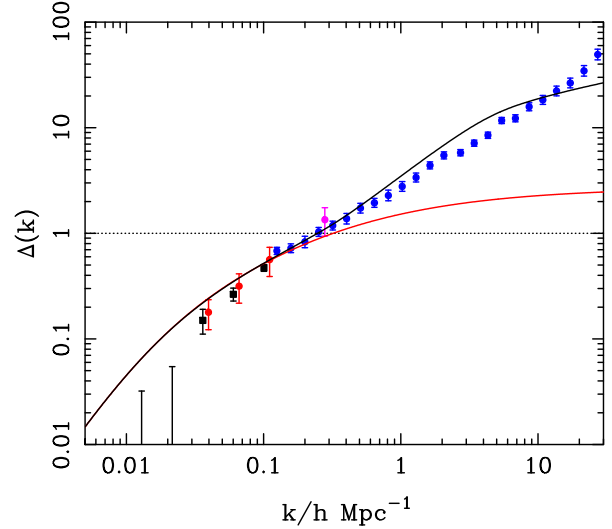


**Figure 2.** The real-space power spectrum of IRAS galaxies. On large, linear scales the analysis of Tadros et al (1999) is used to estimate the real-space band-power in five passbands. On smaller scale we have plotted the real-space power spectrum estimated from the analysis of Saunders et al (1997) from the cross-correlation of the QDOT and QIGC surveys. The lighter points are the mass amplitudes estimated from the redshift space distortion parameter. The last point is the mass amplitude estimated from the abundance of clusters. The model fit is a  $\Lambda$ CDM model with  $\Omega_\Lambda = 0.84$  and  $\Omega_m = 0.16$ ,  $h = 0.65$ . The lighter line is the linear fit, while the solid line uses the nonlinear transformation of Peacock & Dodds (1996).

the velocity dispersion to  $112$  or  $336 \text{km s}^{-1}$ , suggesting that nonlinear effects are not significant for this analysis.

As the amplitude of galaxy perturbations is proportional to the bias factor, we can combine  $\beta$  and the linear galaxy power spectrum to estimate the amplitude of the mass power spectrum,

$$\Delta_m(k) = \beta \Delta_{\text{gal}}(k) \Omega_m^{-0.6}. \quad (9)$$

The real-space power spectrum of the PSCz was estimated by T99, and is plotted in Figure 2. Also shown is the amplitude of mass perturbations for  $\Omega_m = 0.16$ . The point at  $k = 0.23 h\text{Mpc}^{-1}$  is the mass amplitude on a scale of  $8 h^{-1}\text{Mpc}$ , estimated from the abundance of clusters (Henry & Arnaud 1991, White, Efstathiou & Frenk 1993, Viana & Liddle 1996, Eke, Cole & Frenk 1996),

$$\sigma_8 = 0.56 \Omega_m^{-0.47}, \quad (10)$$

with a conservative error of around 30%. The mass amplitude from the PSCz at  $k = 0.1 h\text{Mpc}^{-1}$  is

$$\Delta_m(0.1) = (0.16 \pm 0.04) \Omega_m^{-0.6}. \quad (11)$$

In Figure 2 we plot the mass amplitudes for the PSCz and the cluster abundance. There is a clear consistency between these two estimates of the mass amplitudes. Assuming bias is linear on large scales, estimating mass amplitudes from large-scale redshift surveys is simpler, and hence in principle more robust, than the abundance of clusters argument. In addition this can be used to sample the linear spectrum of mass perturbations on a range of scales, rather than being restricted to one scale.

## 4.2 Cosmological Parameters

Although the shape of the real-space, linear galaxy power spectrum can be used to constrain models of structure formation, the range of points in the linear regime is limited. A better test of models is to compare the mass amplitudes from the PSCz against the amplitude estimated from the CMB. To span the scales between different measurements we need to assume a model linear mass power spectrum. We shall assume that a standard CDM-type power spectrum of the form

$$\Delta_m^2(k) = Q^2 (k/H_0)^4 T^2(k, \Omega_m, h), \quad (12)$$

where we use the CDM transfer function of Bond & Efstathiou (1984), which gives a reasonable fit for a range of CDM models. This provides us with a 3-parameter model dependent on the parameter set  $\Omega_m$ ,  $h$  and  $Q^\dagger$ . This is an interesting parameter set, in particular since CMB data alone cannot constrain  $\Omega_m$  without the addition of LSS data.

If we leave  $h$  as a free parameter, the fit diverges off to high  $h$  and  $Q$  and low  $\Omega_m$ , preserving the shape, but increasing the clustering amplitude. To avoid this we impose the HST constraint that  $h = 0.65 \pm 0.12$ . This effectively removes a degree of freedom in the fit. Beyond this we fit the PSCz mass points, the abundance of clusters constraint and the COBE 4-yr normalisation for a flat universe (Bunn & White 1997);

$$Q = (1.94 \pm 0.2) \times 10^{-5} \Omega_m^{-0.79}. \quad (13)$$

We implicitly assume that the universe is spatially flat, as implied by the recent Boomerang (Lange et al 2000) and MAXIMA (Hanany et al. 2000, Balbi et al. 2000) results and that the spectral index is unity, again as implied by CMB results. We also implicitly assume that the contribution to the mass density from baryons and neutrinos is negligible.

Figure 3 shows the  $\chi^2$  distribution for the  $\Omega_m - Q$  plane, with  $h = 0.65$ . The minimum  $\chi^2$  values are

$$\Omega_m = 0.16 \pm 0.03, \quad Q = (8.4 \pm 3.8) \times 10^{-5} \quad (14)$$

where we quote marginal errors. We can also obtain an estimate of the bias parameter for IRAS galaxies:

$$b = 0.84 \pm 0.28, \quad (15)$$

and the spectral shape parameter,

$$\Gamma = 0.1 \pm 0.03, \quad (16)$$

which is somewhat lower than the usual value of 0.2 from the shape of the galaxy clustering spectrum alone. This best fit has a  $\chi^2 = 2$  for 3 degrees of freedom, and so lies within the range of acceptable fits. However, while suggestive, this analysis makes more assumptions than one would like. These assumptions can be dropped by a combined analysis of the recent Boomerang and MAXIMA results of the small-angle fluctuations in the CMB, which goes beyond our present analysis.

In Figure 2 we plot the PSCz real-space galaxy power spectrum and real-space mass power spectrum, along with

<sup>†</sup> Our parameter  $Q$  is equivalent to the parameter  $\delta_H$ , the amplitude of clustering at the present Hubble scale, used elsewhere.

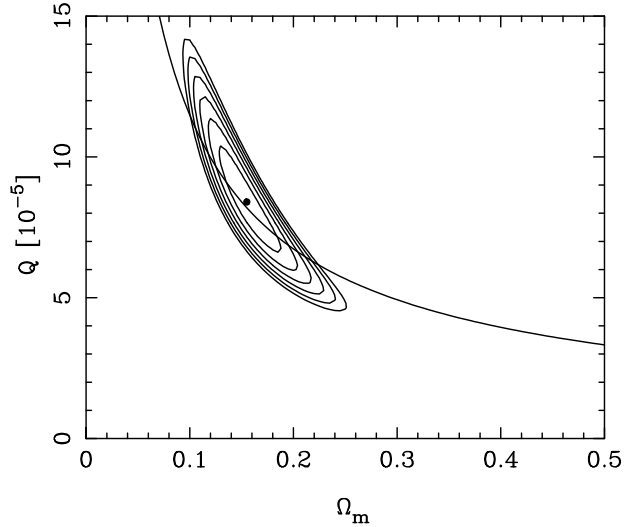


**Figure 3.** The  $\chi^2$  fit to the linear real-space PSCz mass power spectrum, the abundance of clusters and the CMB for the two parameter space of mass-density parameter,  $\Omega_m$ , and the amplitude of mass perturbations,  $Q$ . The solid line is the constraint from the 4-year COBE analysis of the CMB.

our best-fit model, a  $\Lambda$ CDM, normalised to the COBE 4-year data. The model fits over two orders of magnitude in scale, but nonlinear and nonlocal bias effects lead to a disagreement on smaller scales, below  $k = 0.3 h\text{Mpc}^{-1}$ . Recent results from Seljak (2000), Ma & Fry (2000), and Peacock & Smith (2000) suggest that this nonlinear regime can best be understood in terms of a superposition of randomly positioned collapsed clusters, integrated over the cluster mass function. Seljak (2000), and Peacock and Smith (2000) go further to argue that the nonlinear bias function of galaxies arises due to the statistics of the occupation number of galaxies in haloes and show agreement between the  $\Lambda$ CDM model and the small-scale power-law spectrum of galaxies. Perhaps the analysis of this regime is not as daunting as it once appeared.

## 5 CONCLUSIONS

In this paper we have presented a new analysis of the PSCz redshift survey. Using the spherical harmonic analysis of HT, BHT and T99 to decompose the survey, taking into account the effects of linear redshift-space distortions, nonlinear “fingers-of-god” effects, limited sky coverage, and the radial distribution of galaxies in the survey, we have applied a likelihood analysis to a conservative cut of the PSCz survey. The catalogue was cut at 0.75Jy and a conservative mask used to avoid systematic uncertainties at the low-flux end of the catalogue and near the galactic plane. The spherical harmonic analysis of the remaining 7042 galaxies resulted in 4644 harmonic modes. We used a hierarchical data compression to reduce this to 2278 for the final analysis. The compression was applied using a parameter eigenmode approach that compresses information along the line of largest degeneracy in parameter space, thus “squeezing” the uncertainty in this direction.

We used these methods to estimate the redshift-space

distortion parameter,  $\beta$  and the amplitude of the real-space galaxy power spectrum, parameterised by the amplitude,  $\Delta_{0.1}$ , at a wavenumber  $k = 0.1 \text{ hMpc}^{-1}$ . Applying the likelihood analysis to wavenumbers below  $k = 0.2 \text{ hMpc}^{-1}$ , where linear theory will hold and “fingers-of-god” effects can be corrected for, we find

$$\beta = 0.39 \pm 0.12, \quad (17)$$

$$\Delta_{0.1} = 0.42 \pm 0.02 \quad (18)$$

quoting marginalised uncertainties. The distortion parameter is slightly lower than the uncompressed analysis of Tadros et al, with an uncertainty reduced by over a factor of 2. The consistency of these results with that of the earlier analysis of T99 leads us to believe that our analysis has not been heavily contaminated by nonlinear effects, while the conservative cuts in flux and sky coverage avoid contamination by flux systematics. These results also are in agreement with other, independent determinations of the distortion parameter. Comparing the velocity field reconstructed from the PSCz with the ENEAR survey, Nusser et al (2000) find  $\beta = 0.5 \pm 0.1$ , while Valentine, Saunders & Taylor (2000) find  $\beta = 0.5 \pm 0.1$  by comparing the reconstructed dipole with the observed dipole, the bulk flow of galaxies with the MKII survey and the dipole again with the SFI catalogue. Finally, using a least squares fit to the ratios of the galaxy-velocity to galaxy-galaxy and velocity-velocity to galaxy-galaxy power spectra, Hamilton, Tegmark & Padmanabhan find  $\beta = 0.41 \pm 0.13$  for the PSCz.

Since in the linear regime the galaxy power spectrum is likely to be proportional to the mass power spectrum we can combine  $\Delta_{0.1}$  and  $\beta$  to find the amplitude of the mass perturbations,

$$\Delta_m(0.1) = (0.16 \pm 0.04)\Omega_m^{-0.6}. \quad (19)$$

Combined with the constraints from the CMB, and HST observations of the Hubble parameter, and assuming CDM, a flat universe, scale invariant initial mass perturbations and negligible contribution to the total mass-density from baryons and neutrinos we find  $\Omega_m = 0.16 \pm 0.03$ , and a bias parameter for IRAS galaxies of  $b = 0.84 \pm 0.28$ . The minimum  $\chi^2$  fit has a value of  $\chi^2 = 2$  for 3 degrees of freedom.

## ACKNOWLEDGEMENTS

We thank the PSCz team, and especially Will Saunders, for help in understanding the intricacies of the PSCz catalogue. ANT, WEB and HT thank the PPARC for postdoctoral support. Computations were made using STARLINK facilities.

## REFERENCES

- Balbi A., et al., 2000, astro-ph/0005124  
 Ballinger W., 1997, Phd Thesis, Univ. Edinburgh  
 Ballinger W., Heavens A.F., Taylor A.N., 1995, MNRAS, 276, 59p  
 Ballinger W., Taylor A.N., Heavens A.F., Tadros H., 2000, in preparation  
 Bond, J.R., 1995, Phys. Rev. Lett., 74, 4369  
 Bond, J.R., Efstathiou G., 1984, ApJ, 285, L45  
 Bunn E.F., White M., 1997, ApJ, 480, 6  
 Eke V.R., Cole S., Frenk C.S., 1996, MNRAS, 282, 263  
 Feldmann H.A., Kaiser N., Peacock J.A., 1994, ApJ, 426, 23  
 Hanany et al., 2000, astro-ph/0005123  
 Hamilton A.J.S., Tegmark M., Padmanabhan N., 2000, submitted to MNRAS (astro-ph/0004334)  
 Heavens A.F., Taylor A.N., 1995, MNRAS, 275, 483  
 Henry J.P., Arnaud K.A., 1991, ApJ, 372, 410  
 Lange A.E., et al., 2000, astro-ph/0005004  
 Ma C.-P., Fry J.N., 2000, astro-ph/0003343  
 Nusser A., et al, 2000, astro-ph/0006062  
 Padmanabhan N., Tegmark M., Hamilton A., 1999, submitted to ApJ (astro-ph/9911421)  
 Peacock J.A., Dodds S., 1996, MNRAS, 280, L19  
 Peacock J.A., Smith R.E., 2000, astro-ph/0005010  
 Peebles P.J.E., 1980, “Large-Scale Structure of the Universe”, Princeton Univ. Press, Princeton, NJ  
 Saunders W., Rowan-Robinson M., Lawrence A., 1997  
 Saunders W., et al., 2000, astro-ph/0001117  
 Seljak U., 2000, astro-ph/0001493  
 Tadros H., Efstathiou G.P.E., 1996, MNRAS, 282, 1381  
 Tadros H., et al., 1999, MNRAS, 305, 527  
 Taylor et al., 1998, in proc Cambridge Particle Physics and Early Universe Conf. (astro-ph/9707265)  
 Tegmark M., Taylor A.N., Heavens A.F., 1997, ApJ, 480, 22  
 Valentine H., Saunders W., Taylor A.N., 2000, submitted to MNRAS (astro-ph/0006040)  
 Viana P.T., Liddle A.R., 1996, MNRAS, 281, 323  
 White S.D.M., Efstathiou G.P., Frenk C.S., 1993, MNRAS, 262, 1023